

Article

Glutamine Synthetase Contributes to the Regulation of Growth, Conidiation, Sclerotia Development, and Resistance to Oxidative Stress in the Fungus *Aspergillus flavus*

Sen Wang [†], Ranxun Lin [†], Elisabeth Tumukunde , Wanlin Zeng, Qian Bao, Shihua Wang ^{*} and Yu Wang ^{*}

State Key Laboratory of Ecological Pest Control for Fujian and Taiwan Crops, Key Laboratory of Pathogenic Fungi and Mycotoxins of Fujian Province, and School of Life Sciences, Fujian Agriculture and Forestry University, Fuzhou 350002, China

^{*} Correspondence: wshyy1@sina.com (S.W.); wangyu@fafu.edu.cn (Y.W.); Tel.: +86-591-87984471 (S.W.)

[†] These authors contributed equally to the work.

Abstract: The basic biological function of glutamine synthetase (Gs) is to catalyze the conversion of ammonium and glutamate to glutamine. This synthetase also performs other biological functions. However, the roles of Gs in fungi, especially in filamentous fungi, are not fully understood. Here, we found that conditional disruption of glutamine synthetase (AflGsA) gene expression in *Aspergillus flavus* by using a xylose promoter leads to a complete glutamine deficiency. Supplementation of glutamine could restore the nutritional deficiency caused by AflGsA expression deficiency. Additionally, by using the xylose promoter for the downregulation of *AflgsA* expression, we found that AflGsA regulates spore and sclerotic development by regulating the transcriptional levels of sporulation genes *abaA* and *brlA* and the sclerotic generation genes *nsdC* and *nsdD*, respectively. In addition, AflGsA was found to maintain the balance of reactive oxygen species (ROS) and to aid in resisting oxidative stress. AflGsA is also involved in the regulation of light signals through the production of glutamine. The results also showed that the recombinant AflGsA had glutamine synthetase activity in vitro and required the assistance of metal ions. The inhibitor molecule L- α -amino adipic acid suppressed the activity of rAflGsA in vitro and disrupted the morphogenesis of spores, sclerotia, and colonies in *A. flavus*. These results provide a mechanistic link between nutrition metabolism and glutamine synthetase in *A. flavus* and suggest a strategy for the prevention of fungal infection.

Keywords: *Aspergillus flavus* (*A. flavus*); glutamine synthetase; reactive oxygen species (ROS); L- α -amino adipic acid

Key Contribution: AflGsA contributes to the regulation of growth, conidiation, sclerotia development, and resistance to oxidative stress in *A. flavus*. L- α -amino adipic acid suppressed the activity of rAflGsA in vitro and disrupted the morphogenesis of spores, sclerotia, and colonies in *A. flavus*.



Citation: Wang, S.; Lin, R.; Tumukunde, E.; Zeng, W.; Bao, Q.; Wang, S.; Wang, Y. Glutamine Synthetase Contributes to the Regulation of Growth, Conidiation, Sclerotia Development, and Resistance to Oxidative Stress in the Fungus *Aspergillus flavus*. *Toxins* **2022**, *14*, 822. <https://doi.org/10.3390/toxins14120822>

Received: 25 October 2022

Accepted: 21 November 2022

Published: 23 November 2022

Publisher's Note: MDPI stays neutral with regard to jurisdictional claims in published maps and institutional affiliations.



Copyright: © 2022 by the authors. Licensee MDPI, Basel, Switzerland. This article is an open access article distributed under the terms and conditions of the Creative Commons Attribution (CC BY) license (<https://creativecommons.org/licenses/by/4.0/>).

1. Introduction

Aspergillus flavus (*A. flavus*) is a saprophytic, pathogenic, and conditional plant fungus that invades important crops such as peanuts and corn during storage and transportation [1–3]. *A. flavus* is not only a plant pathogenic fungus but also causes invasive aspergillosis, threatening human life [4,5]. In addition, this fungus produces toxic secondary metabolites (aflatoxins) that have been recognized as notorious carcinogenic natural contaminants since their discovery [6–8]. Aflatoxin B1 (AFB1) has strong carcinogenic, teratogenic, and genotoxic properties [9]. Understanding the mechanisms of development and toxin synthesis of *A. flavus* can greatly improve the control strategies for fungal contamination. Therefore, how to effectively prevent and inhibit the infestation of *A. flavus* has become a major challenge.

Nitrogen metabolism is an important part of an organism's metabolism. Glutamine synthetase (Gs) is one of the key central enzymes in the nitrogen metabolic pathway [10] that catalyzes the conversion of glutamate and ammonium to glutamine via an ATP-dependent reaction [11]. Although Gs performs a variety of divergent cellular functions such as nitrogen metabolism and amino acid production [12–15], its biological function is not limited to glutamine synthesis. In wheat (*Triticum aestivum* L.), Gs controls the nitrogen cycle during plant growth and development [16]. Surprisingly, suppression of the Gs gene causes impaired photosynthesis and photorespiration, leading to a significant accumulation of reactive oxygen species (ROS) [17] in *Amaranthus palmeri* (*A. palmeri*). The Gs gene promotes organism repair via cellular nucleotide synthesis after DNA damage [18] and maintains osmotic homeostasis [19]. In *Schizosaccharomyces pombe* (*S. pombe*) and *Aspergillus nidulans* (*A. nidulans*), the inactivation of Gs leads to growth and developmental retardation via glutamine-dependent malnutrition [20,21]. Gs loss of function affects the primary and secondary metabolites' synthesis in the phytopathogenic fungus *Gibberella fujikuroi* (*G. fujikuroi*) [15].

In addition, glutamine synthetase has emerged as a new target for drug discovery and design. Methionine sulfoximine is used as a classical inhibitor for Gs protein activity in bacteria [11]. In plants, the role of Gs makes it an important target for the herbicide glufosinate [22]. Generally, Gs is classified into three types based on molecular weight and 3D spatial structure: GsI, GsII, and GsIII [23]. The Gs-encoding genes in filamentous fungi are usually identified as belonging to the GsII family [24]. Although the amino acid sequences are quite different for the three types of Gs enzymes, these proteins share similar tetrameric geometric structures consisting of two oligomeric rings in a duplex symmetry [25–28]. This oligomerization of Gs indicates that the protein may interact with other molecules and perform their functions in vivo. Indeed, a series of small molecules have been reported to decrease Gs activity, including amino acids, carbamoyl phosphate, and glucosamine-6-phosphate [11,29].

Here, we report that the AflGsA protein is important for colony growth, conidia production, and sclerotia development in *A. flavus*. Furthermore, AflGsA is involved in balancing ROS and resisting oxidative stress. L- α -amino adipic acid, a potent inhibitor of rAflGsA, was effective in inhibiting growth, spore, and sclerotia production in *A. flavus*. These results provide detailed and comprehensive information concerning the regulatory mechanism of AflGsA in *A. flavus*.

2. Results

2.1. Identification of AflGsA in *A. flavus*

The sequence of the *A. flavus* Gs (AflGsA) protein was obtained from the NCBI gene database (AFLA_051930), which exhibited 63% similarity to GsA in *Saccharomyces cerevisiae* (*S. cerevisiae*). All of the analyzed proteins contained two conserved domains (Figure 1A). The phylogenetic tree analysis based on AflGsA and other homologous proteins showed that AflGsA was highly conserved in *Aspergillus* spp. (Figure 1B). The expression profiles of *AflgsA* were monitored by quantitative real-time PCR (qRT-PCR) at vegetative growth (VG), conidial development (CON), aflatoxin synthesis (AS), and sclerotial development (SD) stages [30]. The transcript level of *AflgsA* was the highest in the AS stage, whereas the lowest transcript level was reached in the SD stage (Figure 1C). The differences in expression patterns suggest that *AflgsA* may perform different functions at different stages in *A. flavus*.

2.2. *AflgsA* Is an Essential Gene for the Growth of *A. flavus*

To investigate the function of *AflgsA* in *A. flavus*, we first tried to obtain the *AflgsA* deletion strain by homologous recombination but failed. A better alternative strategy is to construct a xylose promoter mutant strain (^{xyIP}*AflgsA*) for *AflgsA* functional verification (Figure 2A). After confirmation by PCR (Figure 2B) and DNA sequencing (Figure S1), the mutant strain and WT strain were incubated in YXT medium (containing xylose) and

YGT medium (without xylose) for four days at 37 °C in the dark. The mutant strain was completely unable to grow in the xylose-free medium, while growth was partially restored after the addition of xylose (Figure 2C,D). Additionally, a gradient increase in the colony diameter, mycelial tip, and conidial gemination of *xy1^{IP}* *AflgsA* strain was found with an increasing concentration of xylose (Figure S2). These results suggest that glutamine synthetase is essential for the growth of *A. flavus*.

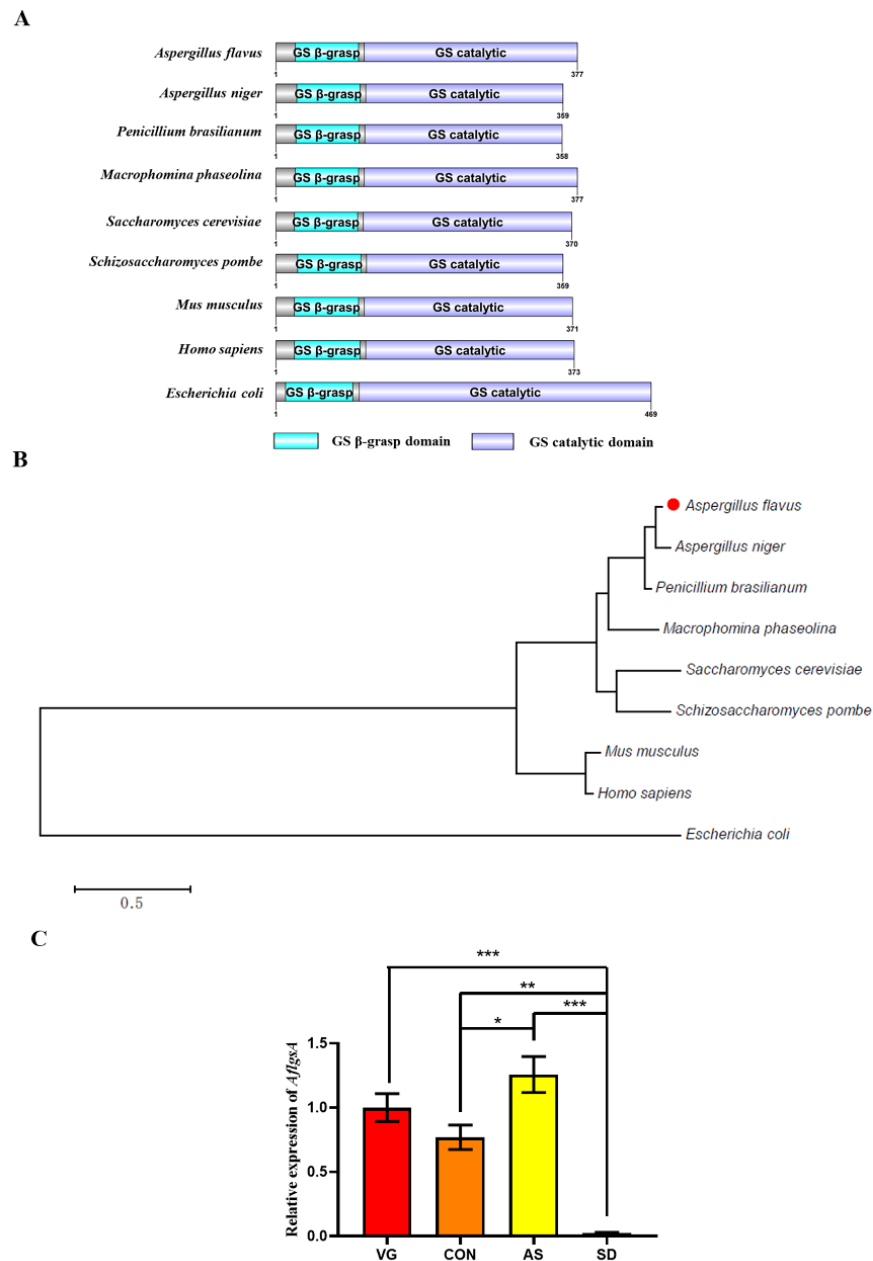


Figure 1. Sequence analysis and expression profiles of *AflGsA* in *A. flavus*. **(A)** Domain structure analysis of *AflGsA* from *A. flavus* and other species (*Aspergillus niger*, *Penicillium brasilianum*, *Macrohomina phaseolina*, *S. cerevisiae*, *S. pombe*, *Mus musculus*, *Homo sapiens*, and *Escherichia coli*). **(B)** Phylogenetic tree of *AflGsA* from different species. **(C)** Expression patterns of *AflgsA* were tested by qRT-PCR at vegetative growth (VG), conidial development (CON), aflatoxin synthesis (AS), and sclerotial development (SD) stages. * indicates a significance level of $p < 0.05$, ** indicates a significance level of $p < 0.01$, and *** indicates a significance level of $p < 0.001$ based on one-way ANOVA with three biological replicates.

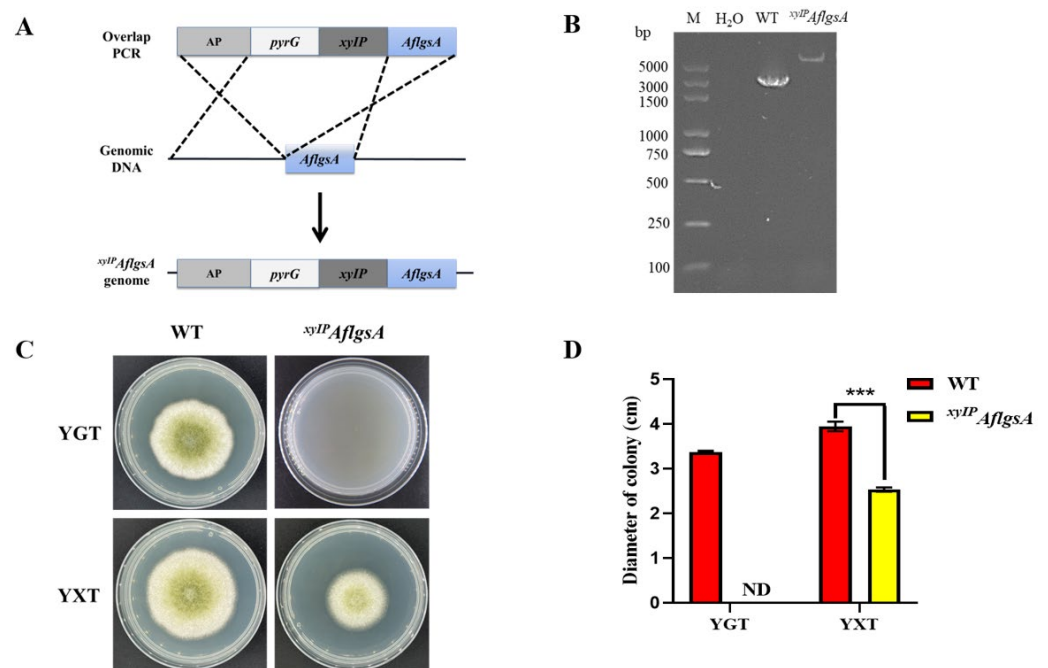


Figure 2. Construction and validation of the *xyIP AflgsA* strain of *A. flavus*. **(A)** The gene replacement strategy for the construction of *xyIP AflgsA*. **(B)** PCR validation of the *xyIP AflgsA* strain. **(C)** Phenotypic observations of the growth for WT and the *xyIP AflgsA* strain in YGT and YXT media in the dark at 37 °C for four days. **(D)** Statistical analysis of the colony diameters of the indicated *A. flavus* strains (panel **C**). ND indicates no detection. *** indicates a significance level of $p < 0.001$ based on *t*-tests with three replicates.

2.3. Glutamine Restores the Growth Defect of the *xyIP AflgsA* Strain

We found that the addition of glutamine (GluN) to the xylose-free or xylose medium restored the growth of the *xyIP AflgsA* strain (Figures 3A,B and S3). Meanwhile, the ammonium tartrate (NH₄⁺) or glutamate (Glu) supplement was unable to promote colony growth (Figures 3A,B and S4). This suggested that the growth defect of the mutant strain was caused by the lack of glutamine synthetase. However, the *xyIP AflgsA* strain showed different colony color compared to the WT strain after GluN supplementation (Figure 3A). Moreover, the growth of the *xyIP AflgsA* strain was also inhibited by adding both GluN and NH₄⁺ (Figure 3B,C). This phenomenon may be due to competition or inhibition of GluN uptake by excess NH₄⁺ [21]. The mechanisms concerning the type of nitrogen sources that mediate the absorption pathway by *AflgsA* in the cell need to be further explored.

2.4. *AflGsA* Is Important for *Conidia* Development of *A. flavus*

To further determine the effect of *AflGsA* on *A. flavus*, we monitored the transcript level of *AflgsA* in the *xyIP AflgsA* strain and found that it was less than half that in the WT (Figure 4A). In addition, the *xyIP AflgsA* strain exhibited smaller spore heads of the child seat and sparser peduncles by microscopic observation (Figure 4B). Statistical analysis also showed a significant reduction in the number of spores in the *xyIP AflgsA* strain compared to that in the WT strain (Figure 4C). Further analysis showed that the transcript levels of both regulatory genes for conidia, *brlA*, and *abaA*, were reduced by about half in the *xyIP AflgsA* strain compared to that in WT (Figure 4D). These results suggest that *AflgsA* may be involved in the upstream regulation of *abaA* and *brlA* genes during spore development of *A. flavus*, and this further regulates the production of conidia.

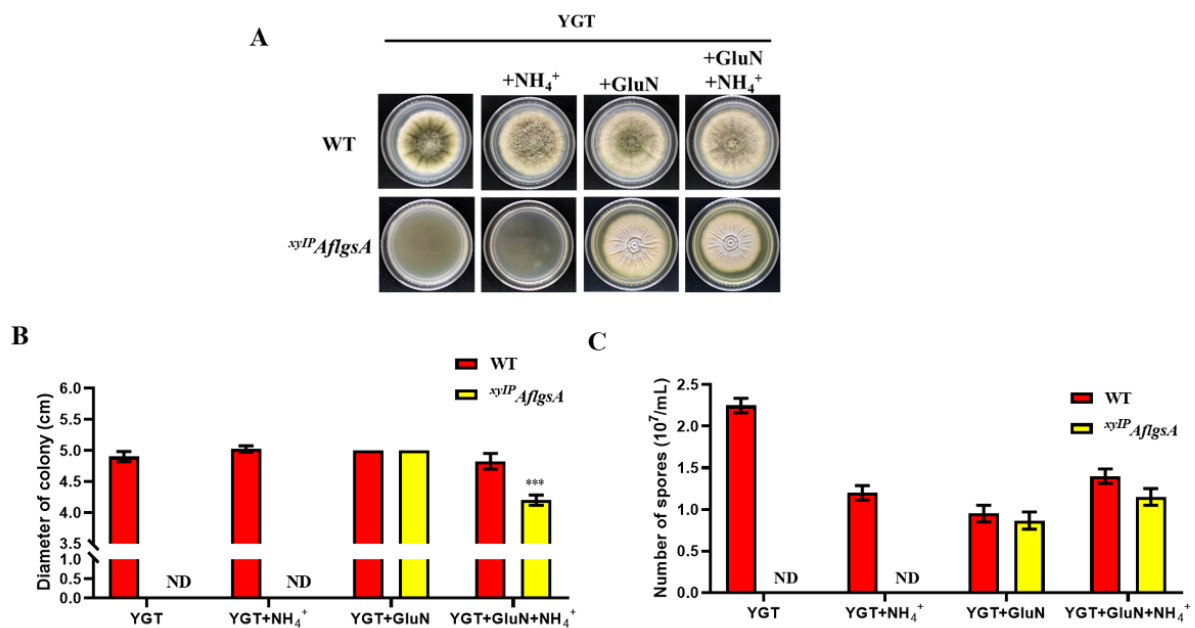


Figure 3. Analysis of the growth of WT and *xyIP AflgsA* strains. (A) The colony morphology of the WT and *xyIP AflgsA* strains on YGT medium containing 10 mM glutamine (GluN) or/and ammonium tartrate (NH₄⁺) as nitrogen sources. (B) Statistical analysis of the diameter from panel (A). (C) The number of conidia produced by the above two *A. flavus* strains. ND indicates no detection. *** indicates a significance level of $p < 0.001$ based on t -tests with three replicates.

2.5. AflGsA Contributes to the Production of Sclerotia but Not to Toxin Synthesis in *A. flavus*

Sclerotia are important reproductive structures of *Aspergillus flavus*, and they aid in survival under harsh conditions. The sclerotia produced by the *xyIP AflgsA* strain were significantly fewer compared to those in the WT strain (Figure 5A,B). In addition, the transcript levels of the sclerotia-related genes *nsdC* and *nsdD* were significantly lower in the *xyIP AflgsA* strain compared to those in the WT strain, only about half of those in the WT strain (Figure 5C). In addition, the sclerotium production defect in the *xyIP AflgsA* strain could not be recovered by the addition of a GluN supplement (Figure S5). These results suggest that AflGsA is important for sclerotia production, and its coding gene may influence sclerotia production by being involved in the upstream regulation of *nsdC* and *nsdD*. We also investigated the production of the toxic secondary metabolite AFB1 in *A. flavus* and found no significant differences in toxin production between the *xyIP AflgsA* strain and the WT (Figure 5D,E). This suggests that AflGsA is not involved in the regulation of aflatoxin production.

2.6. AflGsA Balances ROS and Resists Oxidative Stress in *A. flavus*

A high concentration of ROS causes oxidative damage, disrupting cell metabolism and causing apoptosis. It was found that more ROS were produced in the low-expression state of AflGsA (Figure 6A). When adding hydrogen peroxide to simulate the oxidative stress state, the inhibition rate of the *xyIP AflgsA* strain was significantly higher than that of the WT (Figure 6B,C), but this situation was significantly restored by the addition of GluN (Figure 6B,C). A similar phenotype was also shown in the addition of tBOOH to simulate the oxidative stress state (Figure S6). Further study revealed that there was no significant change in the transcript level of superoxide dismutase gene *sod*. However, the transcript level of the catalase gene *cat* was significantly lower in the *xyIP AflgsA* strain compared to that in the WT strain (Figure 6D). These results suggest that GluN, the catalytic product of AflGsA, plays an important role in resistance to oxidative stress.

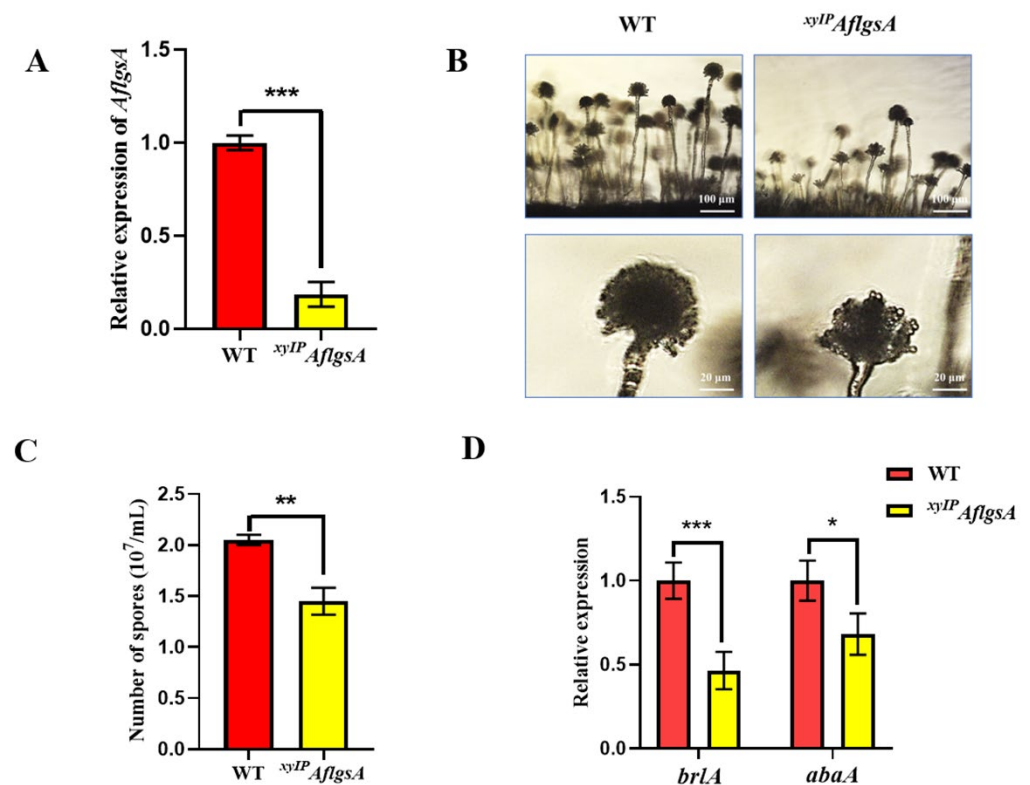


Figure 4. The role of AflGsA in conidia development in *A. flavus*. (A) qRT-PCR analysis of *AflGsA* expression in the WT and *xyIP AflGsA* strains in YXT medium. (B) Microscopic view of conidiophore formation of the above two *A. flavus* strains in YXT medium. (C) The number of conidia produced by the above two *A. flavus* strains in YXT medium. (D) Relative expression of the *brlA* and *abaA* genes in the two above strains in YXT medium with three biological replicates. * indicates a significance level of $p < 0.05$, ** indicates a significance level of $p < 0.01$, and *** indicates a significance level of $p < 0.001$ based on *t*-tests with three biological replicates. The growth conditions of the above strains are described in Sections 5.4 and 5.6.

2.7. AflGsA Is Involved in Light Signaling Pathways in *A. flavus*

The colony diameter of *A. flavus* at 37 °C in the light was significantly smaller than that in the dark (Figure 7A). We also found that the *xyIP AflGsA* strain exhibited significantly higher inhibition rates under light relative to those of the WT strain (Figure 7A,B), but this inhibition of growth was restored with the addition of glutamine (Figure 7A,B). Further studies found that *A. flavus* produced more ROS under light (Figure 7C), indicating that AflGsA could regulate ROS production under light conditions.

2.8. Recombinant AflGsA (rAflGsA) Has Glutamine Synthetase Activity

The recombinant protein rAflGsA (rAflGsA with 6 × His tag, 6 × His-rAflGsA) was successfully expressed and then purified by Ni-NTA column chromatography (Figure 8A). Recombinant protein activity was measured using the classical Gs enzymatic activity assay (see Section 5), and the results showed that rAflGsA has glutamine synthetase activity (Figure 8B). We further analyzed whether divalent metal ions affected the enzyme activity of rAflGsA. Based on the results of activity assays, the highest activity was observed with Mg^{2+} ions (control), while the activities with Mn^{2+} and Ca^{2+} ions were 81% and 72%, respectively (Figure 8C). Glutamine synthetase activity with the addition of Cu^{2+} ions was only 18% (Figure 8C). From the results above, it appears that the activity of rAflGsA requires the assistance of specific metal ions.

2.9. L- α -Amino adipic Acid Is a Potential Inhibitor for rAflGsA and *A. flavus*

L- α -amino adipic acid is a specific gliotoxin in vitro, and this chemical was reported to inhibit Gs activity in rats [31]. In this study, we found that the inhibitor L- α -amino adipic acid suppressed the activity of rAflGsA with an IC₅₀ value of 288.1 μ M in vitro (Figure 8D). The results also showed that L- α -amino adipic acid prevented the growth and conidial germination of *A. flavus* with increasing concentrations (Figures 9A,B and S7). The morphology of conidia was influenced by an increasing concentration, and the spore heads became smaller (Figure 9C). The statistics revealed a gradient decrease in the number of spores of *A. flavus* with an increasing concentration of L- α -amino adipic acid (Figure 9D). When observing the effect of L- α -amino adipic acid on the production of sclerotia, we found a significant decrease in the number of sclerotia when 1.6 mg/mL of L- α -amino adipic acid was added (Figure 9E,F). In contrast, the amount of aflatoxin did not change with an increasing concentration of added L- α -amino adipic acid (Figure 9G,H). In view of the results above, it is clear that L- α -amino adipic acid is an effective inhibitor of rAflGsA and consequently for *A. flavus*. Therefore, we speculate that AflGsA in *A. flavus* is an ideal candidate target for the L- α -amino adipic acid inhibitor.

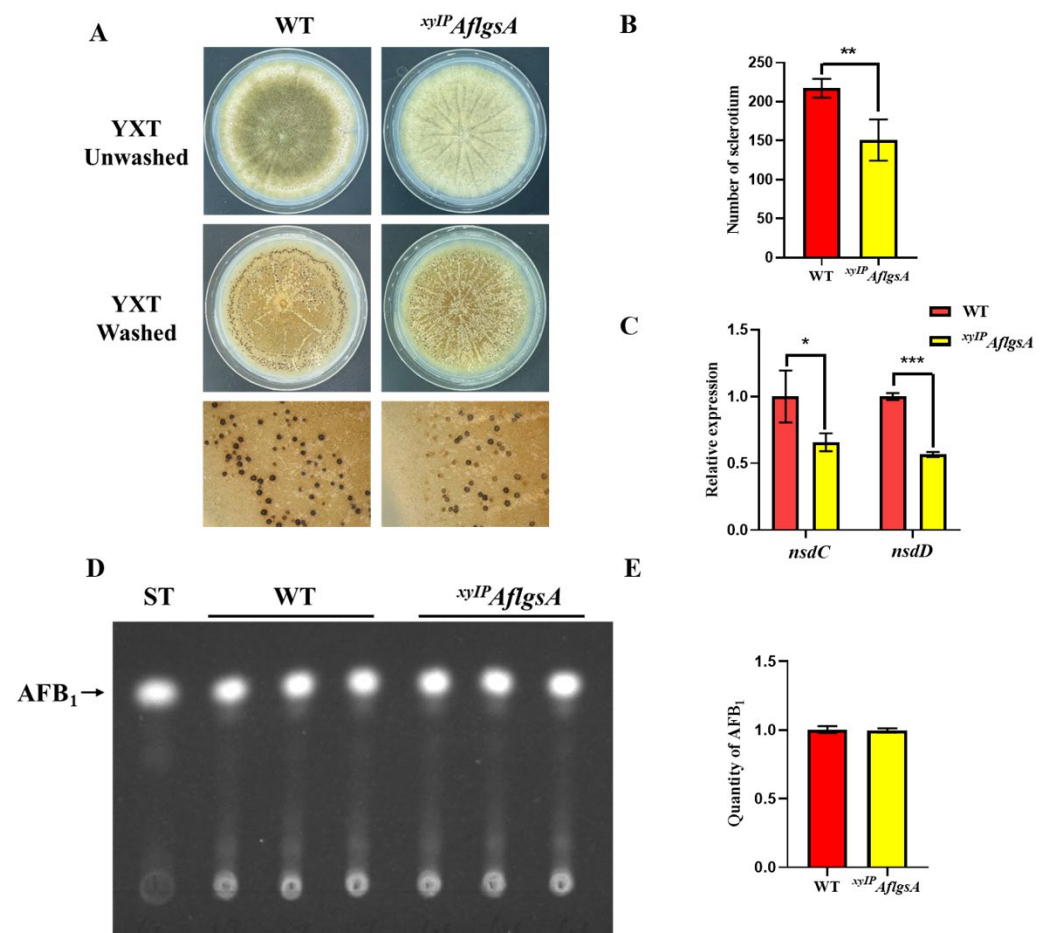


Figure 5. AflGsA regulates sclerotia formation in *A. flavus*. (A) Phenotypic observation of sclerotia formation in WT and *xyIP AflgsA* strains on YXT medium. (B) The number of sclerotia produced by the above two *A. flavus* strains. (C) Relative expression of the *nsdC* and *nsdD* genes in the two strains. (D) TLC analysis of AFB₁ production in *A. flavus* WT and *xyIP AflgsA* strains on YXT medium containing 1 g/L MgSO₄·7H₂O. (E) Optical density analysis of AFB₁ production (as in panel (D)). * indicates a significance level of $p < 0.05$, ** indicates a significance level of $p < 0.01$, and *** indicates a significance level of $p < 0.001$ based on t -tests with three biological replicates.

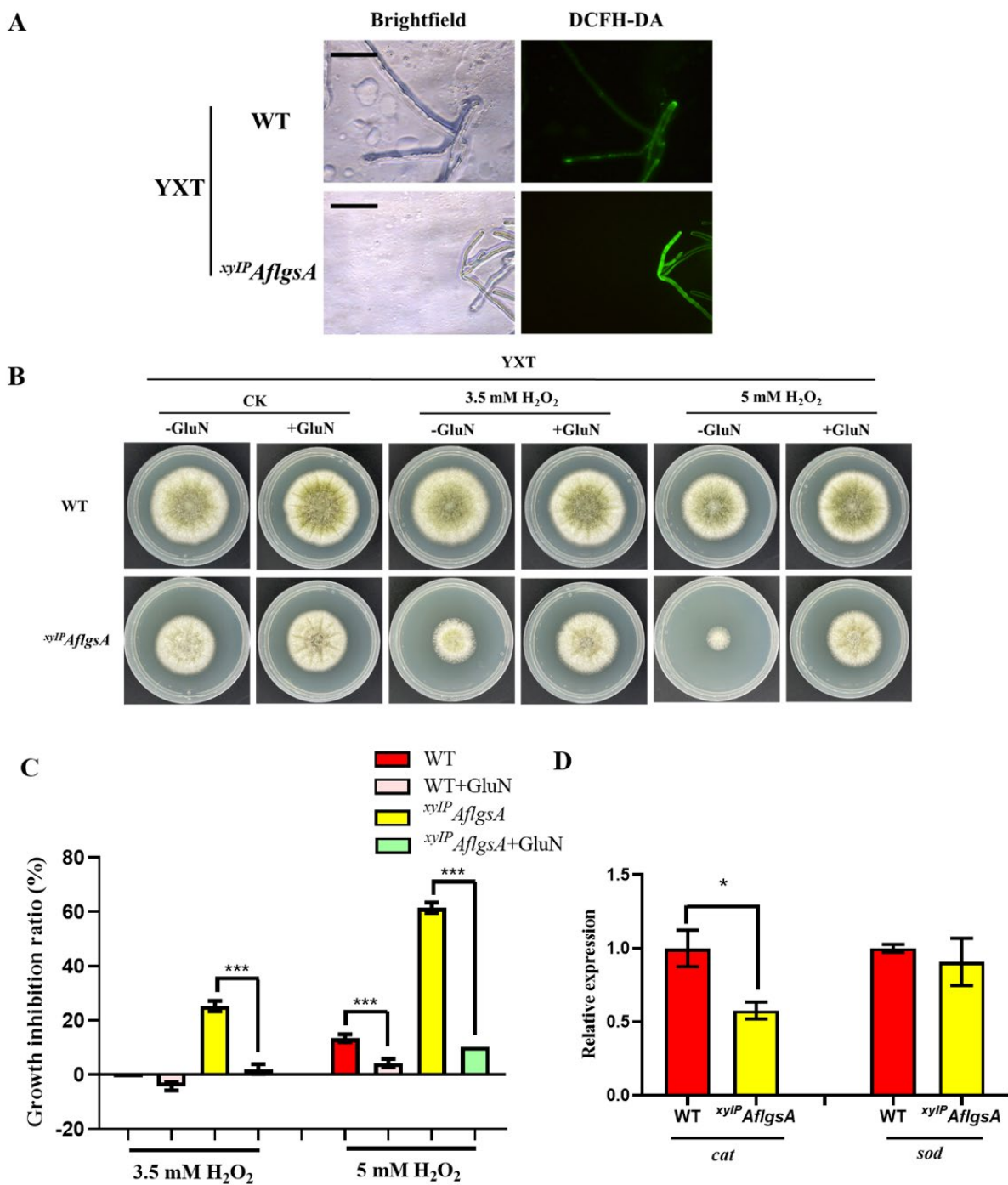


Figure 6. The role of AflGsA in the regulation of ROS and resistance to oxidative stress in *A. flavus*. (A) The ROS content of the WT and *xyIP AflgsA* strains was detected using fluorescence microscopy. (B) Growth phenotype of the WT and *xyIP AflgsA* strains cultured in medium (with or without GluN) with oxidative stress. (C) The growth inhibition rate of different strains in media under oxidative stress (as in panel (B)). *** indicates a significance level of $p < 0.001$ based on one-way ANOVA with three replicates. (D) Relative expression of the *cat* and *sod* genes in the WT and *xyIP AflgsA* strains. * indicates a significance level of $p < 0.05$ based on *t*-tests with three replicates. The growth conditions of the above strains are described in Sections 5.4–5.6.

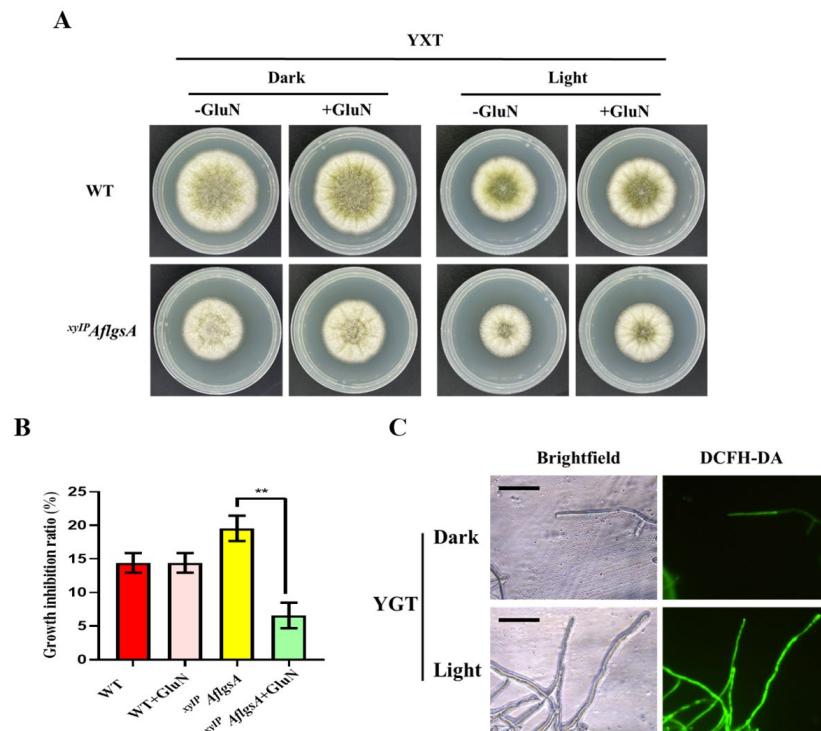


Figure 7. AflGsA is involved in light regulation in *A. flavus*. (A) Growth phenotype of the WT and *xyIP AflGsA* strains cultured in YXT (with GluN or without GluN) in dark or light. (B) Growth inhibition rate of different strains in media with light (panel (A)). (C) ROS content of the WT in dark or light. ** indicates a significance level of $p < 0.01$ based on one-way ANOVA with three replicates.

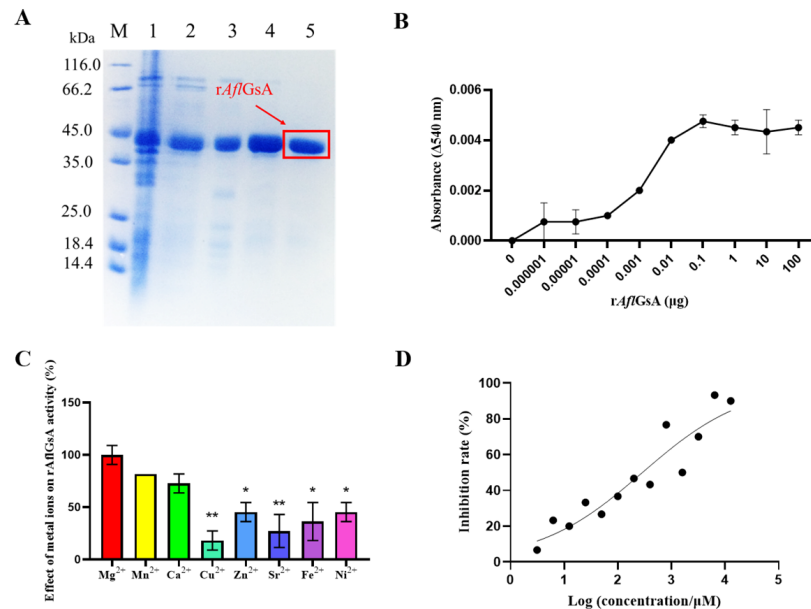


Figure 8. Enzymatic activity assay of recombinant AflGsA. (A) rAflGsA with a 6 \times His label was purified using Ni-NTA column chromatography. Line M: Marker; lane 1: supernatant; lane 2: wash fraction with 50 mM imidazole; lane 3: wash fraction with 100 mM imidazole; lanes 4 and 5: wash fraction with 300 mM imidazole. (B) Enzymatic assay of rAflGsA. (C) Effect of metal ions on rAflGsA activity. The activity assays were performed after incubation of the purified enzymes with 10 mM concentration of different metal chlorides for 30 min. (D) IC₅₀ assay of L- α -amino adipic acid on rAflGsA in vitro. * indicates a significance level of $p < 0.05$, and ** indicates a significance level of $p < 0.01$ based on one-way ANOVA with three biological replicates.

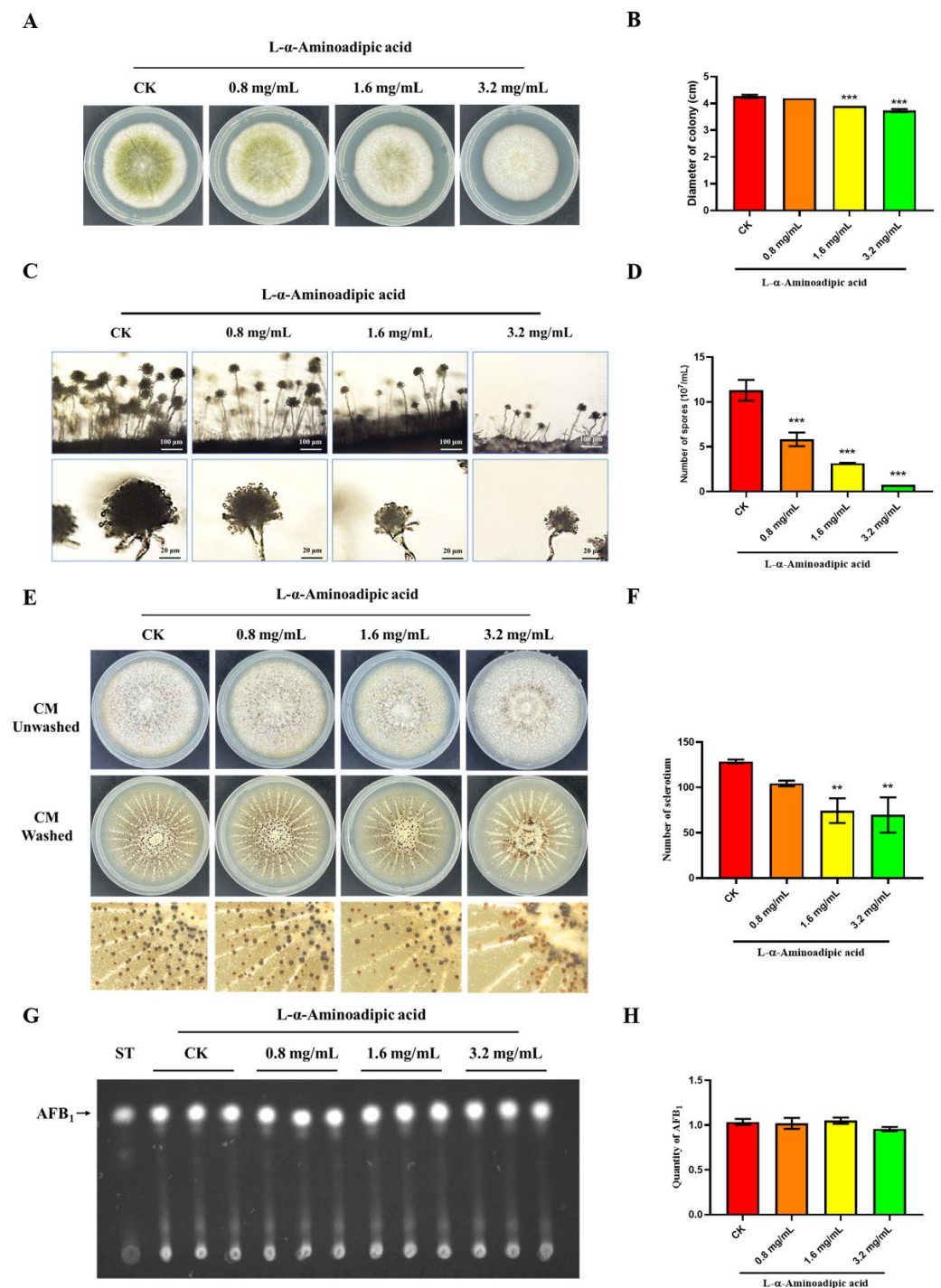


Figure 9. Effect of L- α -aminoadipic acid on growth, conidia production, and sclerotia formation in *A. flavus*. (A) The growth of the *A. flavus* WT strain was inhibited by L- α -aminoadipic acid (0–3.2 mg/mL). (B) Statistical analysis of the colony diameters of the WT strains treated with the inhibitor (as in panel (A)). (C) Microscopic view of conidiophore formation of the WT treated with L- α -aminoadipic acid. (D) The number of conidia produced by the WT strains treated with L- α -aminoadipic acid. (E) Phenotypic observation of sclerotia formation in the WT strains treated with different concentrations of L- α -aminoadipic acid. (F) The number of sclerotia produced by the WT strains (as in panel (E)). (G) TLC analysis of AFB₁ production of the WT strains treated with L- α -aminoadipic acid. (H) Optical density analysis of AFB₁ production (as in panel (G)). ** indicates a significance level of $p < 0.01$, and *** indicates a significance level of $p < 0.001$ based on one-way ANOVA with three biological replicates.

3. Discussion

Glutamine synthetase is responsible for catalyzing the conversion of glutamine from ammonium and glutamate as well as being the central enzyme for nitrogen assimilation [32]. Unlike *Rhizobium meliloti* (*R. meliloti*) [33] and *Magnaporthe oryzae* (*M. oryzae*) [24], which have three Gs proteins, we identified only one putative glutamine synthetase (AflGsA) in *A. flavus*. Furthermore, a previous report on *R. meliloti* stated that only simultaneous knockdown of all three Gs genes could cause a complete glutamine nutritional defect [33]. In *A. flavus*, only one protein has glutamine synthetase activity, and there is no alternative pathway for glutamine synthesis. To study the biofunction of glutamine synthetase in *A. flavus*, we constructed the ^{xyIP}AflgsA mutant strain that has a complete glutamine nutrient-deficient mutation in the YGT medium.

In *A. flavus*, the addition of glutamine to the YGT medium partially restored the growth defect of the ^{xyIP}AflgsA strain. However, in contrast to the pigmented colonies with conidia produced in *A. nidulans* [21], the addition of glutamine to the *A. flavus* mutant strain resulted in the formation of pigmentation defects similar to *M. oryzae* and *G. fujikuroi* [15,24]. This suggests that the glutamine synthetase regulated the production of *A. flavus* pigments, unlike that in *A. nidulans*. In addition, the phenotype after glutamine addition was inhibited by the addition of NH₄⁺, which may be due to the competitive inhibition of GluN by NH₄⁺ [21]. The transcript level of *ghd* gene encoding glutamate dehydrogenase was elevated in the ^{xyIP}AflgsA strain compared to that in WT (Figure S8A). Glutamate dehydrogenase also plays an important role in ammonium assimilation. This may be a balancing mechanism for nitrogen regulation in *A. flavus*.

Like many pathogenic fungi, conidia production and sclerotia formation are important steps in the life cycle of *A. flavus*. It was found that the AflgsA of *A. flavus* plays an important role in the production of conidia. Further results also showed that AflgsA regulates spore production by regulating the transcript levels of the regulatory genes *brlA* and *abaA* for the production of conidia. Similarly to Δ Mogln2 in *M. oryzae* [24], the inhibition of AflgsA function in *A. flavus* was followed by a reduction in the number of conidial peduncles and a smaller head of child seats compared to those in the WT, which may be a reason for the reduction of *A. flavus* spores. In addition, AflgsA in *A. flavus* regulates sclerotia formation by affecting the sclerotia-production-related genes *nsdC* and *nsdD*. All these results suggest that the sophisticated role of AflgsA in multiple developmental stages of *A. flavus* is related to its glutaminyl transferase activity. Glutamine synthetase in *G. fujikuroi* affects the synthesis of gibberellin (GA) and bikaverin metabolites [15]. In contrast, our study showed that both the ^{xyIP}AflgsA mutant and the inhibitor-treated strains produced aflatoxin normally, revealing that AflgsA is not involved in aflatoxin synthesis in *A. flavus*.

ROS is an unavoidable and harmful by-product of oxidative metabolism, and ROS dynamic balance is essential for the development of the fungus [34,35]. The inhibition of glutamine synthetase or light irradiance led to more ROS production and had an inhibitory feedback effect on growth in *A. flavus* that was restored by the addition of glutamine. Photorespiration in plants leads to high production of ROS [36], and inhibition of Gs in *A. palmeri* leads to impaired function of photorespiration accompanied by cell apoptosis [17,22]. Therefore, we hypothesized that glutamine synthetase regulated ROS-mediated inhibition of the growth of *A. flavus* under light conditions. Furthermore, glutamine synthetase can regulate the metabolism in relation to oxidative stress in cyanobacteria [37]. In *M. oryzae*, the Δ Mogln2 strain also results in a high sensitivity to H₂O₂ [24]. In this study, the AflgsA mutant strain of *A. flavus* was highly sensitive to oxidative stress, and this sensitivity was restored by supplementing glutamine. Further studies showed that the transcript level of catalase was significantly reduced in the AflgsA mutant strain, suggesting that the glutamine synthetase pathway resists oxidative stress by regulating the transcriptional level of catalase.

We obtained the rAflGsA protein from *E. coli* with a purity of up to 95% and confirmed that it had glutamate synthase activity. Reports show that glutamine synthetase has positive cooperativity with different cofactors and metal ions [38,39]. Our further study clarified that the glutamine synthesis activity of rAflGsA is dependent on divalent metal ions and that the highest enzyme activity is achieved by the addition of Mg^{2+} and Mn^{2+} ions. This finding was consistent with the results of cation preference towards recombinant glutamine synthetase from *Psychrotrophic Bacterium* [40] and *Mangrove* [41].

L- α -aminoadipic acid is a specific gliotoxin in vitro [42] and is a neuroexcitatory metabolite that reduces extracellular kynurenic acid levels in a dose-dependent manner [43]. However, it is not mentioned in other studies whether L- α -aminoadipic acid has antifungal activity. Our study showed that L- α -aminoadipic acid is an inhibitor for rAflGsA in vitro, and that it also prevents the growth, spore production, and sclerotia formation of *A. flavus* in vivo. In agreement with the phenotype of the *xyIP AflgsA* strain, the addition of L- α -aminoadipic acid had no effect on aflatoxin synthesis. In addition, lower concentrations of L- α -aminoadipic acid (0.8 mg/mL and 1.6 mg/mL) did not affect the transcript level of *AflgsA*, but a higher dosage (3.2 mg/mL) seemed to decrease its transcriptional (Figure S8B). This suggests that L- α -aminoadipic acid may also have other unknown targets in *A. flavus*. Overall, these results suggest that L- α -aminoadipic acid is a potential inhibitor of *A. flavus*, and thus AflGsA may be an ideal target for L- α -aminoadipic acid in *A. flavus*. The study of the inhibition mechanism of L- α -aminoadipic acid against *A. flavus* is important for the prevention of *A. flavus*. This may be a very meaningful research direction in the future.

4. Conclusions

At present, many studies have attempted to elucidate the function of glutamine synthetase in organisms. However, the understanding of the biofunctional diversity of glutamine synthetase in filamentous fungi, especially in *A. flavus*, seems to have been relatively neglected. In this study, we found that AflGsA performed its activity as a glutamine synthetase and that it played a divergent role in the conidia production and sclerotia formation in *A. flavus*. It has an important role in the homeostasis of ROS and resistance to oxidative stress in *A. flavus*. In addition, L- α -aminoadipic acid inhibited both rAflGsA and *A. flavus* and thus was considered as a potential antifungal candidate for further study.

5. Materials and Methods

5.1. Strains and Culture Conditions

E. coli DH5a and BL21 (DE3) were used for plasmid DNA preparation and expression of the recombinant AflGsA (rAflGsA) protein, respectively. *A. flavus* WT and *xyIP AflgsA* strains were cultured in YGT (5 g/L yeast extract, 20 g/L glucose, and 1 mL/L trace elements) and YXT (5 g/L yeast extract, 20 g/L xylose, and 1 mL/L trace elements) media at 37 °C in the dark. Then, 1.5% agar was added to obtain solid media. To study aflatoxin production, YXT medium containing 1 g/L $MgSO_4 \cdot 7H_2O$ was used at 29 °C.

5.2. Sequence Analysis

The NCBI database was used to search for the *AflgsA* sequence of *A. flavus* (AFLA_051930). The homologous protein sequence of AflGsA from *A. flavus* was retrieved by BLAST. The retrieved homologous protein sequences were analyzed by domain analysis using Uniprot Tools and mapped using DOG 2.0 software. The MAGE 7.0 software was used for multiple sequence alignment of the protein sequences, and the maximum likelihood method was used to construct the phylogenetic tree.

5.3. Construction and Identification of Mutant Strain

All of the primers used in this study were shown in Table S1. To obtain the *xyIP AflgsA* mutant strain, we followed the method previously described in the literature [44]. An *AflgsA* xylose promoter mutant cassette was fused by overlapping extension PCR (gsA-

xolap-F and *gsA-xolap-R* primers were used) to an upstream fragment of *AflgsA*, a marker gene (*A. fumigatus pyrG*), the *xyIP* xylose conditional promoter [45], and the *AflgsA* CDS fragment. *A. flavus* CA14 was used as a starting strain during the preparation of protoplasts [46]. The *AflgsA* gene's promoter was converted to a xylose promoter by homologous recombination [44]. The *gsA-A-F* and *gsA-CDS-R* primers were used in the identification of *xyIP AflgsA* transformants by PCR. The *AflgsA-F* and *AflgsA-R* primers were used to identify the sequence by qRT-PCR.

5.4. Analysis of the Growth, Conidial Production, and Sclerotia Formation of *A. flavus*

For colony diameter evaluation, YGT and YXT containing 10 mM glutamine (GluN) or ammonium tartrate (NH_4^+) were points inoculated with 10^6 conidia and incubated in the dark at 37 °C for four days. Spores were eluted with 2 mL of spore eluate and counted under a microscope using a hemocytometer plate to determine the number of spores after incubation in the dark at 37 °C for four days [44]. To observe conidiophore formation, 10^6 conidia were incubated in YXT medium at 37 °C in the dark for two days, and the surface mycelium was scraped off. The colonies were cut out and placed on cover breaks and incubated for 12 h at 37 °C, then observed using a microscope. For sclerotia production analysis, 10^6 conidia were incubated in YXT medium at 37 °C in the dark for seven days, and the morphology of sclerotia was recorded by rinsing off the mycelium with 75% ethanol [47]. For aflatoxin extraction, 10^6 conidia were incubated in YXT containing 1 g/L $\text{MgSO}_4 \cdot 7\text{H}_2\text{O}$ at 29 °C in the dark for five days. The toxin in the medium was extracted using chloroform and detected using TLC [44].

5.5. Detection of ROS in *A. flavus*

To detect the ROS in *A. flavus*, WT and *xyIP AflgsA* strains were incubated in YXT liquid medium at 37 °C for 24 h. Mycelia were washed three times with a phosphate-buffered saline (PBS) buffer. The collected mycelia were incubated with a 10 μM DCFH-DA fluorescent probe (Beyotime, Nantong, China) for 30 min at 37 °C. After washing three times with PBS, the mycelium was placed on a slide, and ROS content was identified by microscopy. Fluorescence emission of DCFH-DA was excited at 488 nm.

5.6. Quantitative Real-Time PCR

The mycelia of the strains of *A. flavus* were collected after 48 h of incubation. The collected mycelia were ground in liquid nitrogen, and total RNA was extracted with the TRIzol (Biomarker Technologies, Beijing, China) reagent. RNA was translated into cDNA using a reverse transcription kit (Thermo Scientific, Waltham, MA, USA). The cDNA was then used as a template for quantitative PCR with specific primers [48].

5.7. Purification of Recombinant rAflGsA Protein and Determination of Enzyme Activity

The cDNA of *AflgsA* from *A. flavus* was expanded and cloned into the pET-28a expression vector. The expressed recombinant AflGsA (rAflGsA) protein was purified using Ni-NTA column chromatography [44]. The activity of rAflGsA was then measured at 540 nm using the classical glutamine synthetase enzyme activity assay [40]. Different divalent metal ions were added to assay the enzyme activity with a final concentration of 20 mM. Enzyme activity was measured after reacting at 37 °C for one hour.

5.8. Statistical Analysis

GraphPad Prism 5.0 (GraphPad Software, San Diego, CA, USA) was used for data statistics and analysis. All of the analyses had at least three biological replicates if not specifically indicated.

Supplementary Materials: The following supporting information can be downloaded at: <https://www.mdpi.com/article/10.3390/toxins14120822/s1>, Table S1: Oligonucleotide primers used in this study; Figure S1: Genome sequencing validation of the *xyIP AflgsA* strain of *A. flavus*. *AflgsA* AP is the upstream noncoding region of the *AflgsA* gene. The mutations in the *AflgsA* CDS are synonymous mutations; Figure S2: Analysis of the growth, mycelial morphology, conidial germination, and conidiophore formation of WT and *xyIP AflgsA* strains. (A) The mycelial morphology of WT and *xyIP AflgsA* strains on the medium containing 10 g/L and 20 g/L xylose. (B) The colony morphology of WT and *xyIP AflgsA* strains. (C) Statistical analysis of the diameter from panel (B). (D) Conidial germination of WT and *xyIP AflgsA* strains. (E) Statistical analysis of the conidial germination rate from panel (D). (F) Microscopic view of the conidiophore formation of the above two *A. flavus* strains. (G) The number of conidia produced by the above two *A. flavus* strains. ND indicates no detection. ** indicates a significance level of $p < 0.01$, and *** indicates a significance level of $p < 0.001$ based on *t*-tests with three replicates. The medium containing 10 g/L xylose: 5 g/L yeast extract, 10 g/L glucose, 10 g/L xylose, 1 mL/L trace elements, and 1.5% agar. The medium containing 20 g/L xylose (YXT medium): 5 g/L yeast extract, 20 g/L xylose, 1 mL/L trace elements, and 1.5% agar; Figure S3: Analysis of the growth of WT and *xyIP AflgsA* strains. (A) The colony morphology of the WT and *xyIP AflgsA* strains on YXT medium containing 10 mM glutamine (GluN) or/and ammonium tartrate (NH_4^+) as nitrogen sources. (B) Statistical analysis of the diameter from panel (A). *** indicates a significance level of $p < 0.001$ based on *t*-tests with three replicates; Figure S4: Analysis of the growth of WT and *xyIP AflgsA* strains. (A) The colony morphology of the WT and *xyIP AflgsA* strains on YGT medium containing 10 mM glutamate (Glu) or on YXT medium. (B) Statistical analysis of the diameter from panel (A). ND indicates no detection. *** indicates a significance level of $p < 0.001$ based on *t*-tests with three replicates; Figure S5: AflGsA regulates sclerotia formation in *A. flavus*. (A) Phenotypic observation of sclerotia formation in WT and *xyIP AflgsA* strains on YXT medium containing 10 mM glutamine (GluN). (B) The number of sclerotia produced by the above two *A. flavus* strains. ND indicates no detection. * indicates a significance level of $p < 0.05$ based on *t*-tests with three replicates; Figure S6: The role of AflGsA in resistance to oxidative stress in *A. flavus*. (A) Growth phenotype of the WT and *xyIP AflgsA* strains cultured in medium (with or without GluN) with 0.8 mM tBOOH oxidative stress. (B) The growth inhibition rate of different strains in media under oxidative stress (as in panel (A)). *** indicates a significance level of $p < 0.001$ based on one-way ANOVA with three replicates; Figure S7: Effect of L- α -amino adipic acid on mycelial morphology and conidial germination in *A. flavus*. (A) The mycelial morphology of the *A. flavus* WT strain was inhibited by L- α -amino adipic acid (0–3.2 mg/mL). (B) The conidial germination of the *A. flavus* WT strain was inhibited by L- α -amino adipic acid (0–3.2 mg/mL). (C) Statistical analysis of the conidial germination rate from panel B. ND indicates no detection. * indicates a significance level of $p < 0.05$, ** indicates a significance level of $p < 0.01$, and *** indicates a significance level of $p < 0.001$ based on one-way ANOVA with three replicates; Figure S8: Relative expression of the genes in different strains. (A) Relative expression of the *ghd* gene in the WT and *xyIP AflgsA* strains. (B) Relative expression of the *AflgsA* gene of the WT strains treated with the inhibitor. * indicates a significance level of $p < 0.05$ based on *t*-tests or one-way ANOVA with three replicates.

Author Contributions: Conceptualization, S.W. and Y.W.; formal analysis, R.L.; funding acquisition, S.W. (Shihua Wang) and Y.W.; methodology, S.W. (Sen Wang); project administration, S.W. (Shihua Wang); supervision, S.W. (Shihua Wang) and Y.W.; validation, S.W. (Sen Wang), R.L., W.Z. and Q.B.; visualization, Y.W.; writing—original draft, S.W. (Sen Wang); writing—review and editing, E.T., S.W. (Shihua Wang) and Y.W. All authors have read and agreed to the published version of the manuscript.

Funding: This research was funded by the Scientific Research Foundation of the Graduate School of Fujian Agriculture and Forestry University (324-1122yb054) and the Science and Technology Innovation Fund of Fujian Agriculture and Forestry University (CXZX2020051A).

Institutional Review Board Statement: Not applicable.

Informed Consent Statement: Not applicable.

Data Availability Statement: Not applicable.

Conflicts of Interest: The authors declare no conflict of interest.

References

1. Bennett, J.W.; Klich, M.A. *Aspergillus*: Biology and industrial applications. *Biotechnology* **1992**, *23*, 1.
2. Samson, R.A. Current taxonomic schemes of the genus *Aspergillus* and its teleomorphs. *Biotechnology* **1992**, *23*, 355–390.
3. Amaike, S.; Keller, N.P. *Aspergillus flavus*. *Annu. Rev. Phytopathol.* **2011**, *49*, 107–133. [[CrossRef](#)] [[PubMed](#)]
4. Krishnan, S.; Manavathu, E.K.; Chandrasekar, P.H. *Aspergillus flavus*: An emerging non-fumigatus *Aspergillus* species of significance. *Mycoses* **2009**, *52*, 206–222. [[CrossRef](#)] [[PubMed](#)]
5. Kousha, M.; Tadi, R.; Soubani, A.O. Pulmonary aspergillosis: A clinical review. *Eur. Respir. Rev. Off. J. Eur. Respir. Soc.* **2011**, *20*, 156–174. [[CrossRef](#)]
6. Mehl, H.L.; Jaime, R.; Callicott, K.A.; Probst, C.; Garber, N.P.; Ortega-Beltran, A.; Grubisha, L.C.; Cotty, P.J. *Aspergillus flavus* diversity on crops and in the environment can be exploited to reduce aflatoxin exposure and improve health. *Ann. N. Y. Acad. Sci.* **2012**, *1273*, 7–17. [[CrossRef](#)]
7. Lim, C.W.; Yoshinari, T.; Layne, J.; Chan, S.H. Multi-mycotoxin screening reveals separate occurrence of aflatoxins and ochratoxin a in Asian rice. *J. Agric. Food Chem.* **2015**, *63*, 3104–3113. [[CrossRef](#)]
8. Leung, M.C.; Díaz-Llano, G.; Smith, T.K. Mycotoxins in pet food: A review on worldwide prevalence and preventative strategies. *J. Agric. Food Chem.* **2006**, *54*, 9623–9635. [[CrossRef](#)]
9. Choi, K.C.; Chung, W.T.; Kwon, J.K.; Yu, J.Y.; Jang, Y.S.; Park, S.M.; Lee, S.Y.; Lee, J.C. Inhibitory effects of quercetin on aflatoxin B1-induced hepatic damage in mice. *Food Chem. Toxicol. Int. J. Publ. Br. Ind. Biol. Res. Assoc.* **2010**, *48*, 2747–2753. [[CrossRef](#)]
10. Lam, H.M.; Coschigano, K.T.; Oliveira, I.C.; Melo-Oliveira, R.; Coruzzi, G.M. The molecular-genetics of nitrogen assimilation into amino acids in higher plants. *Annu. Rev. Plant Physiol. Plant Mol. Biol.* **1996**, *47*, 569–593. [[CrossRef](#)]
11. Eisenberg, D.; Gill, H.S.; Pfluegl, G.M.; Rotstein, S.H. Structure-function relationships of glutamine synthetases. *Biochim. Biophys. Acta* **2000**, *1477*, 122–145. [[CrossRef](#)]
12. Christa, L.; Simon, M.T.; Flinois, J.P.; Gebhardt, R.; Brechot, C.; Lasserre, C. Overexpression of glutamine synthetase in human primary liver cancer. *Gastroenterology* **1994**, *106*, 1312–1320. [[CrossRef](#)]
13. Caizzi, R.; Bozzetti, M.P.; Caggese, C.; Ritossa, F. Homologous nuclear genes encode cytoplasmic and mitochondrial glutamine synthetase in *Drosophila melanogaster*. *J. Mol. Biol.* **1990**, *212*, 17–26. [[CrossRef](#)]
14. Avisar, N.; Shiftan, L.; Ben-Dror, I.; Havazelet, N.; Vardimon, L. A silencer element in the regulatory region of glutamine synthetase controls cell type-specific repression of gene induction by glucocorticoids. *J. Biol. Chem.* **1999**, *274*, 11399–11407. [[CrossRef](#)]
15. Teichert, S.; Schönig, B.; Richter, S.; Tudzynski, B. Deletion of the *Gibberella fujikuroi* glutamine synthetase gene has significant impact on transcriptional control of primary and secondary metabolism. *Mol. Microbiol.* **2004**, *53*, 1661–1675. [[CrossRef](#)]
16. Kichey, T.; Le Gouis, J.; Sangwan, B.; Hirel, B.; Dubois, F. Changes in the cellular and subcellular localization of glutamine synthetase and glutamate dehydrogenase during flag leaf senescence in wheat (*Triticum aestivum* L.). *Plant Cell Physiol.* **2005**, *46*, 964–974. [[CrossRef](#)]
17. Takano, H.K.; Beffa, R.; Preston, C.; Westra, P.; Dayan, F.E. A novel insight into the mode of action of glufosinate: How reactive oxygen species are formed. *Photosynth. Res.* **2020**, *144*, 361–372. [[CrossRef](#)]
18. Fu, S.; Li, Z.; Xiao, L.; Hu, W.; Zhang, L.; Xie, B.; Zhou, Q.; He, J.; Qiu, Y.; Wen, M.; et al. Glutamine Synthetase Promotes Radiation Resistance via Facilitating Nucleotide Metabolism and Subsequent DNA Damage Repair. *Cell Rep.* **2019**, *28*, 1136–1143. [[CrossRef](#)]
19. Kim, C.; Kültz, D. An osmolality/salinity-responsive enhancer 1 (OSRE1) in intron 1 promotes salinity induction of tilapia glutamine synthetase. *Sci. Rep.* **2020**, *10*, 12103. [[CrossRef](#)]
20. Sasaki, Y.; Kojima, A.; Shibata, Y.; Mitsuzawa, H. Filamentous invasive growth of mutants of the genes encoding ammonia-metabolizing enzymes in the fission yeast *Schizosaccharomyces pombe*. *PLoS ONE* **2017**, *12*, e0186028. [[CrossRef](#)]
21. Margelis, S.; D’Souza, C.; Small, A.J.; Hynes, M.J.; Adams, T.H.; Davis, M.A. Role of glutamine synthetase in nitrogen metabolite repression in *Aspergillus nidulans*. *J. Bacteriol.* **2001**, *183*, 5826–5833. [[CrossRef](#)] [[PubMed](#)]
22. Takano, H.K.; Dayan, F.E. Biochemical Basis for the Time-of-Day Effect on Glufosinate Efficacy against *Amaranthus palmeri*. *Plants* **2021**, *10*, 2021. [[CrossRef](#)] [[PubMed](#)]
23. Rodríguez-Herrero, V.; Payá, G.; Bautista, V.; Vegara, A.; Cortés-Molina, M.; Camacho, M.; Esclapez, J.; Bonete, M.J. Essentiality of the *glnA* gene in *Haloferax mediterranei*: Gene conversion and transcriptional analysis. *Extrem. Life Extrem. Cond.* **2020**, *24*, 433–446. [[CrossRef](#)]
24. Aron, O.; Wang, M.; Lin, L.; Batool, W.; Lin, B.; Shabbir, A.; Wang, Z.; Tang, W. MoGLN2 Is Important for Vegetative Growth, Conidiogenesis, Maintenance of Cell Wall Integrity and Pathogenesis of *Magnaporthe oryzae*. *J. Fungi* **2021**, *7*, 463. [[CrossRef](#)] [[PubMed](#)]
25. Almassy, R.J.; Janson, C.A.; Hamlin, R.; Xuong, N.H.; Eisenberg, D. Novel subunit—Subunit interactions in the structure of glutamine synthetase. *Nature* **1986**, *323*, 304–309. [[CrossRef](#)]
26. Valentine, R.C.; Shapiro, B.M.; Stadtman, E.R. Regulation of glutamine synthetase. XII. Electron microscopy of the enzyme from *Escherichia coli*. *Biochemistry* **1968**, *7*, 2143–2152. [[CrossRef](#)]
27. van Rooyen, J.M.; Abratt, V.R.; Belrhali, H.; Sewell, T. Crystal structure of Type III glutamine synthetase: Surprising reversal of the inter-ring interface. *Structure* **2011**, *19*, 471–483. [[CrossRef](#)]

28. Chen, Y.; Xu, W.; Yu, S.; Ni, K.; She, G.; Ye, X.; Xing, Q.; Zhao, J.; Huang, C. Assembly status transition offers an avenue for activity modulation of a supramolecular enzyme. *eLife* **2021**, *10*, e72535. [[CrossRef](#)]
29. Woolfolk, C.A.; Stadtman, E.R. Regulation of glutamine synthetase: III. Cumulative feedback inhibition of glutamine synthetase from *Escherichia coli*. *Arch. Biochem. Biophys.* **1967**, *118*, 736–755. [[CrossRef](#)]
30. Lan, H.; Wu, L.; Sun, R.; Keller, N.P.; Yang, K.; Ye, L.; He, S.; Zhang, F.; Wang, S. The HosA histone deacetylase regulates aflatoxin biosynthesis through direct regulation of aflatoxin cluster genes. *Mol. Plant-Microbe Interact.* **2019**, *32*, 1210–1228. [[CrossRef](#)]
31. McBean, G.J. Inhibition of the glutamate transporter and glial enzymes in rat striatum by the gliotoxin, alpha amino adipate. *Br. J. Pharmacol.* **1994**, *113*, 536–540. [[CrossRef](#)]
32. Bao, A.; Zhao, Z.; Ding, G.; Shi, L.; Xu, F.; Cai, H. The Stable Level of Glutamine synthetase 2 plays an important role in Rice growth and in Carbon-Nitrogen metabolic balance. *Int. J. Mol. Sci.* **2015**, *16*, 12713–12736. [[CrossRef](#)]
33. Shatters, R.G.; Liu, Y.; Kahn, M.L. Isolation and characterization of a novel glutamine synthetase from *Rhizobium meliloti*. *J. Biol. Chem.* **1993**, *268*, 469–475. [[CrossRef](#)]
34. Aguirre, J.; Ríos-Momberg, M.; Hewitt, D.; Hansberg, W. Reactive oxygen species and development in microbial eukaryotes. *Trends Microbiol.* **2005**, *13*, 111–118. [[CrossRef](#)]
35. Gessler, N.N.; Aver'yanov, A.A.; Belozerskaya, T.A. Reactive oxygen species in regulation of fungal development. *Biochem. Biokhimiia* **2007**, *72*, 1091–1109. [[CrossRef](#)]
36. Apel, K.; Hirt, H. Reactive oxygen species: Metabolism, oxidative stress, and signal transduction. *Annu. Rev. Plant Biol.* **2004**, *55*, 373–399. [[CrossRef](#)]
37. Robles-Rengel, R.; Florencio, F.J.; Muro-Pastor, M.I. Redox interference in nitrogen status via oxidative stress is mediated by 2-oxoglutarate in cyanobacteria. *New Phytol.* **2019**, *224*, 216–228. [[CrossRef](#)]
38. Montanini, B.; Betti, M.; Márquez, A.J.; Balestrini, R.; Bonfante, P.; Ottonello, S. Distinctive properties and expression profiles of glutamine synthetase from a plant symbiotic fungus. *Biochem. J.* **2003**, *373*, 357–368. [[CrossRef](#)]
39. Sakakibara, H.; Shimizu, H.; Hase, T.; Yamazaki, Y.; Takao, T.; Shimonishi, Y.; Sugiyama, T. Molecular identification and characterization of cytosolic isoforms of glutamine synthetase in maize roots. *J. Biol. Chem.* **1996**, *271*, 29561–29568. [[CrossRef](#)]
40. Gong, C.; You, X.; Zhang, S.; Xue, D. Functional analysis of a glutamine biosynthesis protein from a psychrotrophic Bacterium, *Cryobacterium soli* GJ02. *Indian J. Microbiol.* **2020**, *60*, 153–159. [[CrossRef](#)]
41. Zhao, W.; Yang, J.; Tian, Y.; Fu, X.; Zhu, B.; Xue, Y.; Gao, J.; Han, H.J.; Peng, R.; Yao, Q.H. Expression, purification, and characterization of recombinant mangrove glutamine synthetase. *Mol. Biol. Rep.* **2014**, *41*, 7575–7583. [[CrossRef](#)] [[PubMed](#)]
42. Huck, S.; Grass, F.; Hörtnagl, H. The glutamate analogue alpha-amino adipic acid is taken up by astrocytes before exerting its gliotoxic effect *in vitro*. *J. Neurosci. Off. J. Soc. Neurosci.* **1984**, *4*, 2650–2657. [[CrossRef](#)] [[PubMed](#)]
43. Wu, H.Q.; Ungerstedt, U.; Schwarcz, R. L-alpha-amino adipic acid as a regulator of kynurenic acid production in the hippocampus: A microdialysis study in freely moving rats. *Eur. J. Pharmacol.* **1995**, *281*, 55–61. [[CrossRef](#)] [[PubMed](#)]
44. Wang, Y.; Wang, S.; Nie, X.; Yang, K.; Xu, P.; Wang, X.; Liu, M.; Yang, Y.; Chen, Z.; Wang, S. Molecular and structural basis of nucleoside diphosphate kinase-mediated regulation of spore and sclerotia development in the fungus *Aspergillus flavus*. *J. Biol. Chem.* **2019**, *294*, 12415–12431. [[CrossRef](#)]
45. Zadra, I.; Abt, B.; Parson, W.; Haas, H. *xylP* promoter-based expression system and its use for antisense downregulation of the *Penicillium chrysogenum* nitrogen regulator NRE. *Appl. Environ. Microbiol.* **2000**, *66*, 4810–4816. [[CrossRef](#)]
46. Chang, P.K.; Scharfenstein, L.L.; Wei, Q.; Bhatnagar, D. Development and refinement of a high-efficiency gene-targeting system for *Aspergillus flavus*. *J. Microbiol. Methods* **2010**, *81*, 240–246. [[CrossRef](#)]
47. Zhang, F.; Geng, L.; Deng, J.; Huang, L.; Zhong, H.; Xin, S.; Fasoyin, O.E.; Wang, S. The MAP kinase AflSl2 modulates aflatoxin biosynthesis and peanut infection in the fungus *Aspergillus flavus*. *Int. J. Food Microbiol.* **2020**, *322*, 108576. [[CrossRef](#)]
48. Yang, K.; Liu, Y.; Wang, S.; Wu, L.; Xie, R.; Lan, H.; Fasoyin, O.E.; Wang, Y.; Wang, S. Cyclase-associated protein Cap with multiple domains contributes to mycotoxin biosynthesis and fungal virulence in *Aspergillus flavus*. *J. Agric. Food Chem.* **2019**, *67*, 4200–4213. [[CrossRef](#)]